Hindawi Publishing Corporation
International Journal of Antennas and Propagation
Volume 2015, Article ID 851904, 9 pages
http://dx.doi.org/10.1155/2015/851904

Research Article

A Novel Metamaterial MIMO Antenna with High Isolation for WLAN Applications

Nguyen Khac Kiem,[1] Huynh Nguyen Bao Phuong,[2] Quang Ngoc Hieu,[3] and Dao Ngoc Chien[4]

[1] *Hanoi University of Science and Technology, Hanoi 100000, Vietnam*
[2] *Quy Nhon University, Binh Dinh 820000, Vietnam*
[3] *Chuo University, Tokyo 1920393, Japan*
[4] *Ministry of Science and Technology, Hanoi 100000, Vietnam*

Correspondence should be addressed to Nguyen Khac Kiem; kiem.nguyenkhac@hust.edu.vn

Received 11 September 2014; Revised 24 December 2014; Accepted 8 January 2015

Academic Editor: Xinyi Tang

A compact 2 × 2 metamaterial-MIMO antenna for WLAN applications is presented in this paper. The MIMO antenna is designed by placing side by side two single metamaterial antennas which are constructed based on the modified composite right/left-handed (CRLH) model. By adding another left-handed inductor, the total left-handed inductor of the modified CRLH model is increased remarkably in comparison with that of conventional CRLH model. As a result, the proposed metamaterial antenna achieves 60% size reduction in comparison with the unloaded antenna. The MIMO antenna is electrically small (30 mm × 44 mm) with an edge-to-edge separation between two antennas of $0.06\lambda_0$ at 2.4 GHz. In order to reduce the mutual coupling of the antenna, a defected ground structure (DGS) is inserted to suppress the effect of surface current between elements of the proposed antenna. The final design of the MIMO antenna satisfies the return loss requirement of less than −10 dB in a bandwidth ranging from 2.38 GHz to 2.5 GHz, which entirely covers WLAN frequency band allocated from 2.4 GHz to 2.48 GHz. The antenna also shows a high isolation coefficient which is less than −35 dB over the operating frequency band. A good agreement between simulation and measurement is shown in this context.

1. Introduction

Recently, social demand on multimedia communication has been rapidly increasing resulting in development of modern wireless communication systems such as Wi-Fi, WiMAX, and 3G/4G. Along with these applications, modern antennas are required to have small size and light weight. However, the typical antennas are usually large in size due to the operating wavelength, so they are difficult to meet the requirements of modern antennas. There are several techniques used to decrease the size of antenna, such as incorporating a shorting pin in a microstrip patch [1], using short circuit [2], and cutting slots in radiating patch [3, 4], by partially filled high permittivity substrate [5] or by Fractal microstrip patch configuration [6]. Besides, transmission line metamaterial (TL-MM) [7] is one of the methods that provides a conceptual way for implementing small resonant antenna [8–15]. The first proposals of using TL-MM structures at resonance to implement small sprinted antennas have been documented in [9, 10].

Wireless LANs have experienced phenomenal growth during the past several years. The new WLANs standard (IEEE 802.11n) promises both higher data rates and increases reliability. This standard is based on MIMO communication technology which has received much attention as a practical method to substantially increase wireless channel capacity without additional power and spectrum. A multiple antenna system is needed for MIMO system. However, it is difficult to integrate two or more antennas in a mobile device. There are two critical factors for MIMO antenna system. One is total size of antenna system with a limited space of mobile device. In such a way the antenna elements must be compact and

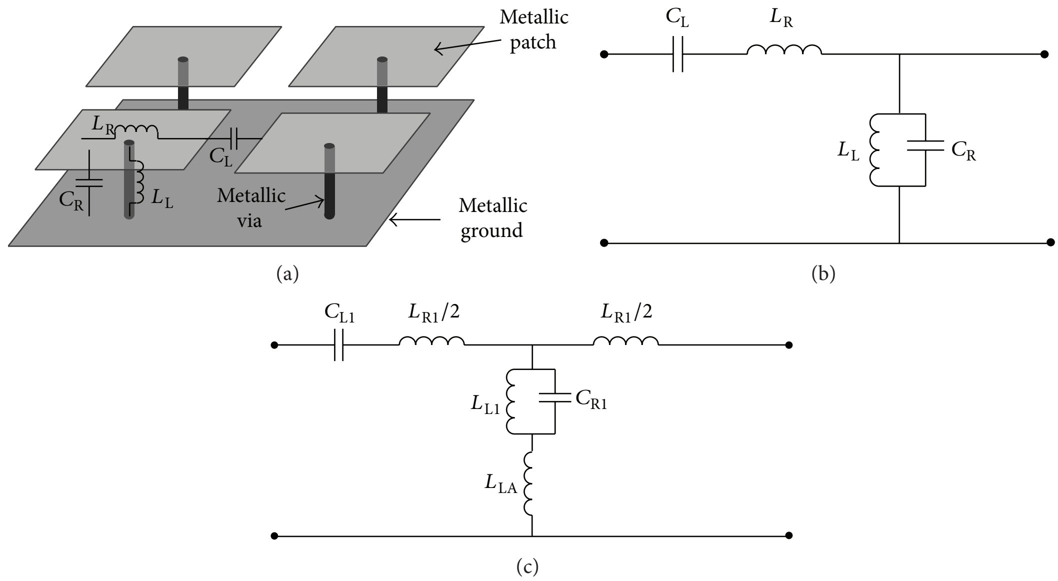

FIGURE 1: CRLH transmission line: (a) mushroom-like EBG model, (b) equivalent circuit of unit cell, and (c) equivalent circuit of proposed metamaterial antenna.

be put very close. The other factor is the isolation between antenna elements. Due to the close space between antenna elements, the coupling coefficient among radiating elements is very high. This will degrade the performance of MIMO system. Therefore, it will be a real challenging task to design a MIMO antenna with small size while obtaining a very high isolation coefficient.

In this paper, a very compact metamaterial MIMO antenna is proposed. The MIMO antenna consists of two antennas which are based on composite left/right handed (CLRH) transmission lines for reducing the antenna dimension. In the proposed configuration, a defected ground structure (DGS) is employed to increase the isolation between two antenna elements. Thus, a novel metamaterial MIMO antenna is proposed which has a high isolation with only 7.5 mm ($0.06\lambda_0$) distance between antenna elements. This antenna is built on a FR4 substrate with total volume of $30 \times 44 \times 1.6\,\text{mm}^3$ and has very compact radiating elements with total size of $8.92 \times 32.6\,\text{mm}^2$ and operates at the frequency band of 2.38–2.5 GHz while the values of isolation coefficients are below −35 dB over operating frequency band.

The rest of this paper is organized as follow. In Section 2, detailed designs of the single metamaterial antenna are presented. The proposed MIMO antenna is then introduced in both cases of initial and final design. The simulated and measured results are shown in Section 3, while some conclusions are provided in Section 4.

2. Design of Metamaterial MIMO Antenna

In this work, the design of the antenna is divided into two parts. In the first one, a metamaterial antenna is designed for WLAN frequency ranging from 2.4 GHz to 2.48 GHz. In the second part, the two identical single metamaterial antennas are utilized as elements to form a 2×2 MIMO antenna. Finally, the defected ground structure is implemented to diminish the mutual coupling of the antennas.

2.1. Design of Single Metamaterial Antenna. The configuration of metamaterial antenna is shown in Figure 2(a). The antenna is printed on a low-cost FR4 substrate with the thickness of 1.6 mm, dielectric constant ε of 4.4, and loss tangent $\tan\delta$ of 0.02. As a reference comparison, an unloaded microstrip fed rectangular strip with the length of l_1 is chosen as the monopole radiating element. In order to maintain compact electrical length while decreasing the operating frequencies, the monopole antenna is constructed by a modified CRLH single-cell.

The model of conventional CRLH transmission line is shown in Figure 1(a). This is a mushroom-like EBG which can be interpreted by equivalent circuit depicted in Figure 1(b). From this figure, the serial left-handed (LH) capacitor (C_L) is created by two adjacent metallic patches placed on the top surface of the structure while the shunt LH inductor (L_L) created by the current flows from the metallic patch to ground plane through metallic via. Moreover, the serial right-handed (RH) inductor (L_R) is formed by the metallic patch and the shunt RH capacitor (C_R) is created due to the parallel arrangement of metallic patch and ground plane.

The equivalent circuit of proposed metamaterial antenna is shown in Figure 1(c). In this design, the metamaterial-loading is carried out in an asymmetric fashion, where serial LH capacitor (C_{L1}) is formed between two strips separated by a distance s_1 (as shown in Figure 2(a)) while the shunt LH inductor (L_{L1}) is formed similarly to the shunt LH one shown in Figure 1(b). Moreover, the additional LH inductor (L_{LA}) is built up by meandered strips which connect the structure and the ground plane. Regarding RH components, the serial RH inductor (L_{R1}) is formed by the main patch with length of l_1 and shunt RH capacitor (C_{R1}) is formed similarly

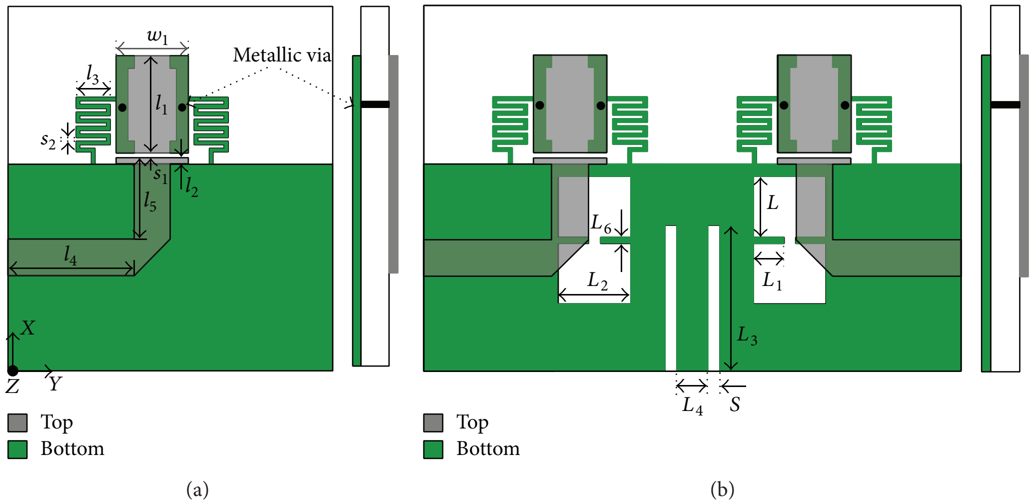

Figure 2: Configuration of the proposed antennas: (a) single metamaterial antenna and (b) metamaterial MIMO antenna.

Table 1: Dimensions of single metamaterial antenna.

l_1	8 mm	l_4	10.5 mm	s_1	0.42 mm
l_2	0.5 mm	l_5	6.7 mm	s_2	0.3 mm
l_3	2.8 mm	w_1	6 mm		

Table 2: Dimensions of metamaterial MIMO antenna.

L	5 mm	L_3	12 mm	S	2.5 mm
L_1	2.5 mm	L_4	1 mm		
L_2	6 mm	L_6	0.5 mm		

to the RH components of conventional CRLH model. As a result, a single metamaterial antenna is proposed with the size of radiating element of 8.92 × 12.6 mm^2 ($0.07\lambda_0 \times 0.1\lambda_0$ at 2.4 GHz) and printed in a substrate with two dimensions of 27 × 30 mm^2. Finally, the center resonant frequency of proposed metamaterial antenna is defined as follows:

$$f_C = \frac{1}{2\pi\sqrt{(L_{L1} + L_{LA})\,C_{R1}}}. \quad (1)$$

2.2. Design of Metamaterial MIMO Antenna. In this design, a MIMO model is constructed by placing two single antennas side by side at the distance of 20 mm ($0.16\lambda_0$ at 2.4 GHz) from center-to-center or 7.5 mm ($0.06\lambda_0$ at 2.4 GHz) from edge-to-edge, making the overall the dimension of this design very compact. The layout of the MIMO antenna is shown in Figure 2(b). In order to increase the isolation between elements of MIMO antenna, a defected ground structure is etched in a part of ground between two elements. Firstly, two parallel slots are etched on the ground plane. As a result, the MIMO antenna satisfies the isolation requirement while the operating frequencies were shifted compared to the WLAN frequency band. Therefore, two I-shaped slots which are used as an impedance matching circuit are etched on the metallic ground (as shown in Figure 2(b)). The final MIMO antenna system is proposed with total size of radiating elements of 8.92 × 32.6 mm^2 and satisfies all requirements of MIMO system with very high isolation between antenna elements. All the dimensions of the proposed single metamaterial antenna and MIMO antenna are given in Tables 1 and 2, respectively.

3. Results and Discussions

The performance of the proposed antennas is discussed in detail in terms of simulation and measurement results.

3.1. Single Metamaterial Antenna. As mentioned in Section 2, the resonant frequency of proposed metamaterial antenna depends on the meandered strip length which is controlled by tuning the length l_3 as well as the gap between strip steps s_2. The simulated S_{11} results of the single metamaterial antenna with different values of l_3 and s_2 are shown in Figure 3. In Figure 3, the resonant frequency reduces with the increasing the value of l_3 and s_2. Actually, the increase of l_3 and s_2 will lead to the increase of the additional LH inductor L_{LA} and therefore making the decrease of the resonant frequency. This is entirely consistent with formula (1). The optimized bandwidth is obtained when the l_3 and s_2 are set at 2.8 mm and 0.3 mm, respectively. It can be seen from Figure 7 that the bandwidth of the antenna defined by the S_{11} less than −10 dB entirely covers the WLAN frequency range, which is allocated from 2.4 to 2.48 GHz.

The size reduction of the proposed antenna is carried out by taking the simulated S_{11} of antennas in case of loaded (proposed antenna) and unloaded (conventional antenna). The two antennas are given the same dimensions of substrate layer and radiation elements. As can be seen from Figure 4, the resonant frequency of the unloaded antenna centers at 6 GHz while the resonant one of the proposed antenna is maintained at 2.44 GHz. It is clear that the proposed antenna exhibits smaller resonant frequency than the conventional one. In this case, the proposed antenna achieves 60% size reduction in comparison with the conventional one.

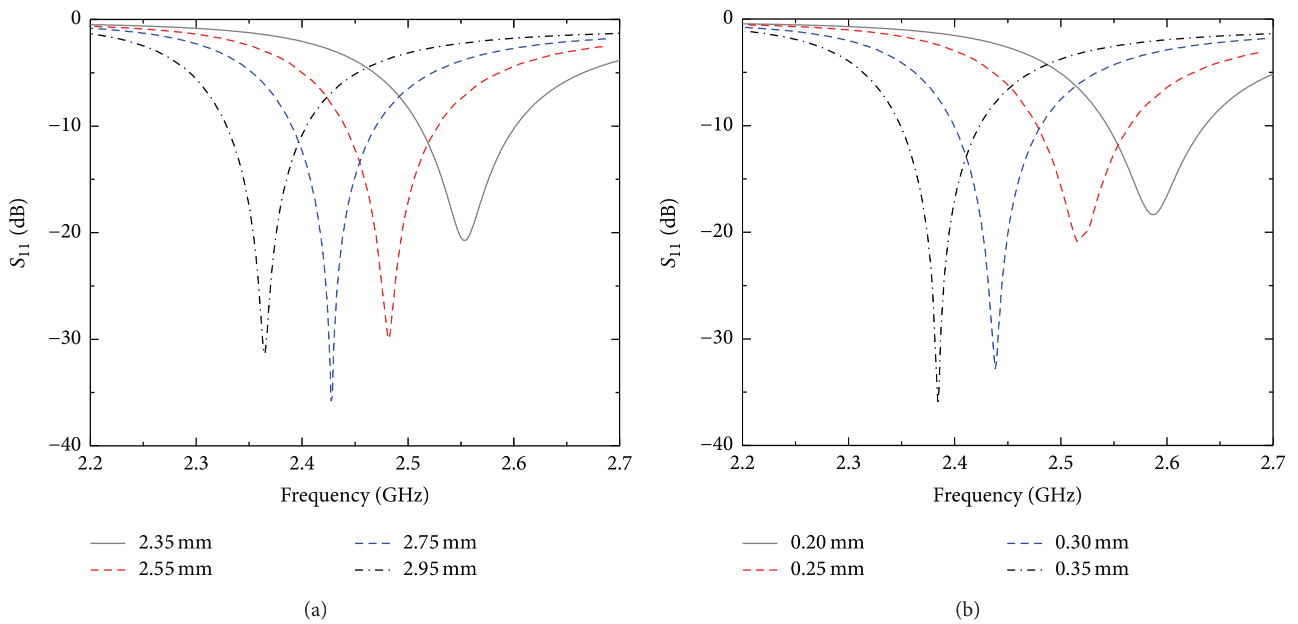

FIGURE 3: Simulated S_{11} of single metamaterial antenna for different values of (a) l_3 and (b) s_2.

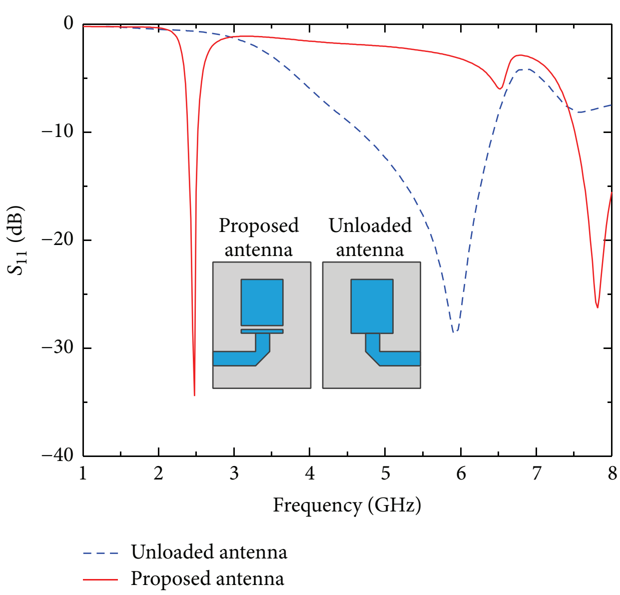

FIGURE 4: Simulated S_{11} of unloaded and proposed antennas.

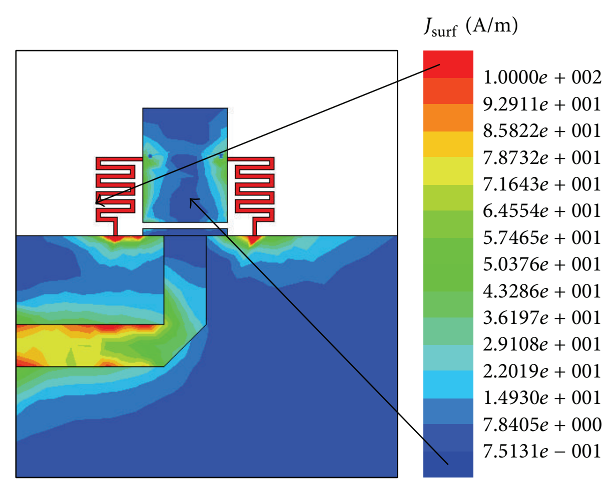

FIGURE 5: Surface current distribution on single antenna at 2.44 GHz.

Current distributions of the metamaterial antenna at the center frequency of WLAN are exhibited in Figure 5. As observed in Figure 5, the current distribution on antenna at 2.44 GHz mainly focuses on the meandered strips instead of on the radiating patch as the principle of microstrip antenna.

The radiation pattern of single antenna at the center frequency of 2.44 GHz is plotted in Figure 6. The solid lines display the E-plane and the dotted lines represent H-plane. It can be observed that the single antenna possesses an isotropic radiation pattern confirming its operation in the fundamental resonant mode. Therefore, its gain is small with the maximum total gain of 1.4 dB.

Finally, the fabricated single metamaterial antenna is presented in Figure 13. The simulated and measured results of S_{11} of single metamaterial antenna is shown in Figure 7. From this figure, it can be observed that the antenna can operate over the range spreading from 2.4 GHz to 2.48 GHz and from 2.405 GHz to 2.495 GHz in simulation and measurement, respectively.

3.2. Metamaterial MIMO Antenna. The simulated results of reflection coefficients of the initial MIMO antenna (without DGS) are shown in Figure 8. From this figure, it is observed that the initial antenna does not satisfy the impedance

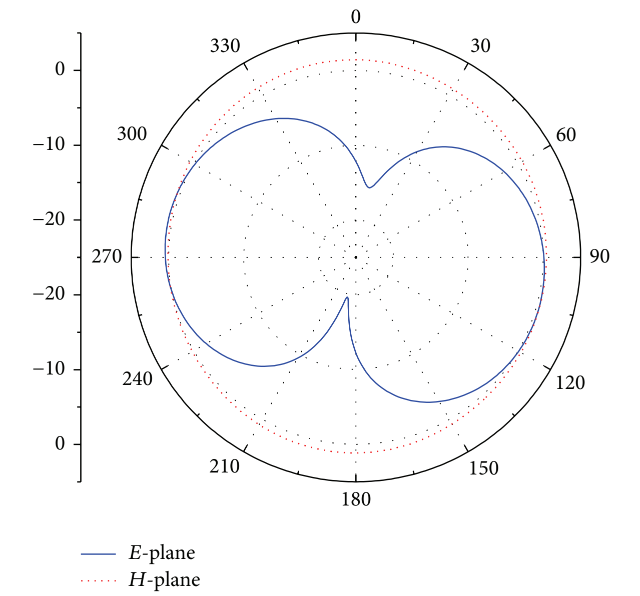

FIGURE 6: Simulated radiation pattern of single metamaterial antenna at center frequency of 2.44 GHz.

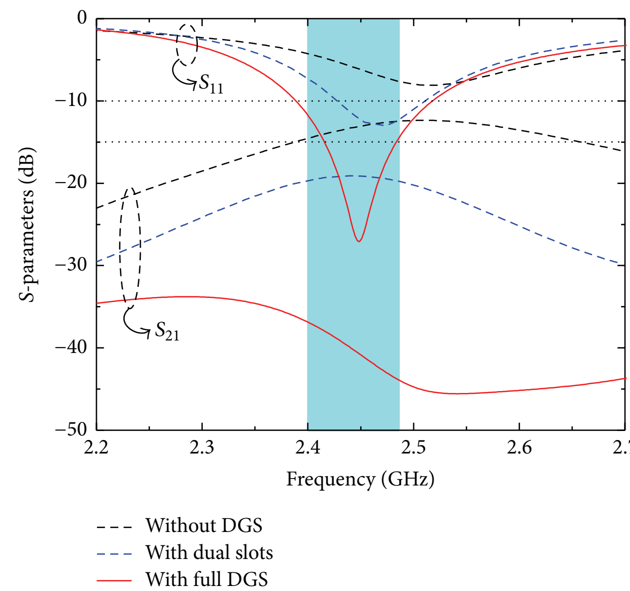

FIGURE 8: Simulated S-parameters in three cases: without DGS, with dual slots, and with full DGS.

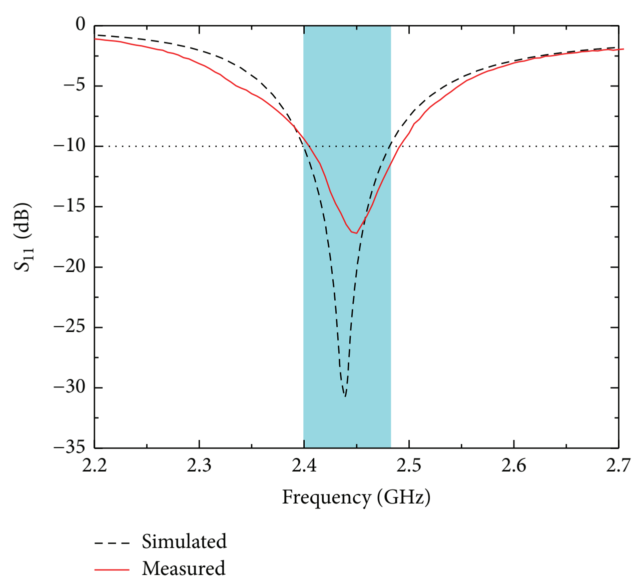

FIGURE 7: Simulated and measured results of single metamaterial antenna.

matching condition due to the effect of mutual coupling. The S-parameters of antenna are changed and could not meet the requirements of MIMO antenna from which S_{11} and S_{22} are not below −10 dB and S_{21} and S_{12} are not below −15 dB in WLAN band. This fact is clearly demonstrated by the surface current distribution on the initial MIMO antenna in Figure 10(a). As can be observed from Figure 10(a), when the first element (Port 1) is excited, the surface current is strongly induced on the second element (Port 2) resulting in a rise of the mutual coupling (S_{21} and S_{12}). Actually, the mutual coupling can be reduced by increasing the distance between the elements. However, this will lead to the larger size of the proposed MIMO antenna. These drawbacks of the initial MIMO antenna can be solved thanks to the use of defected ground structure etched on the common ground of MIMO antenna by the following two steps.

At first, two parallel slots are added to central ground plane between two ports (as shown in Figure 2(b)). The length slot L_3 is varied to find out the value from which the impedance matching and mutual coupling have the best solution. The optimized length of L_3 is chosen as 12 mm. Simulated S-parameters of MIMO antenna with dual slots are shown in Figure 8. From this figure, it can be seen that the isolation coefficient S_{21} is lower than −18 dB for all frequency in WLAN band. However, the impedance is not matched enough in this band so that the S_{11} is below −10 dB over the frequency ranging from 2.42 GHz to 2.5 GHz, and therefore the antenna could not cover the WLAN frequencies.

The current distribution of MIMO antenna with the implementation of dual slots at 2.44 GHz is shown in Figure 10(b). It can be seen from Figure 10(b) that the surface current partly focuses on the slots and somewhat coupling to the radiation strips of the adjacent antenna element.

In order to solve this problem, in the second step, two I-shaped slots are etched on the ground plane and used as an impedance matching circuit. The effect of I-shaped slots to impedance matching of the MIMO antenna is investigated via the length L. Figure 9 shows the simulated S-parameters of the MIMO antenna for the different values of L. It can be observed that the isolation coefficient is below −15 dB for all cases and the return loss is changed with the various sizes of slots. When the length L of I-slots increases, the input impedance decreases make the impedance highly matched. The final MIMO antenna with full DGS is formed as the value of L fixed at 5 mm. As a result, the full DGS MIMO

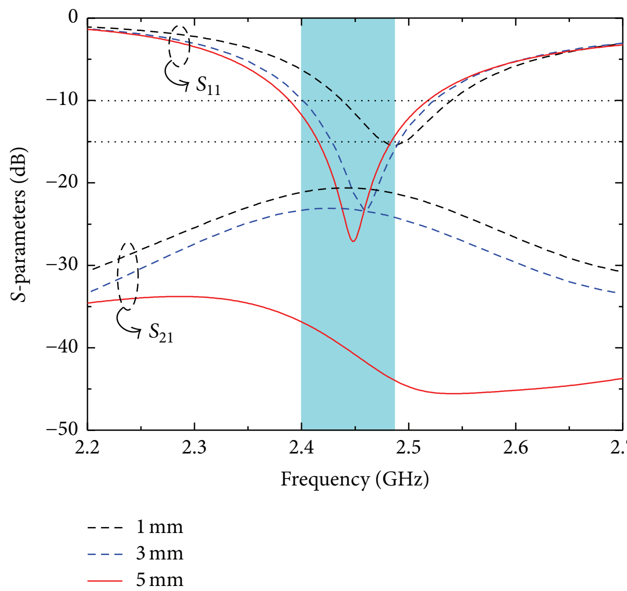

FIGURE 9: Simulated S-parameters of full DGS MIMO antenna for different values of L.

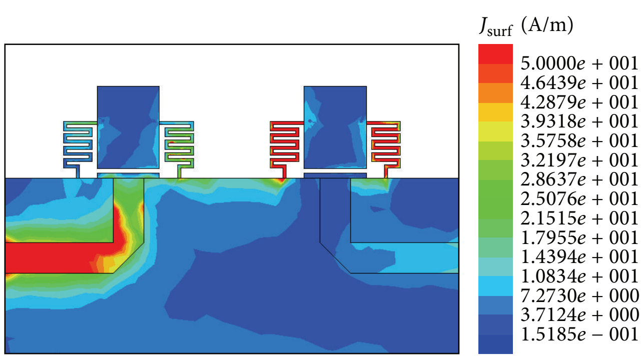

(a)

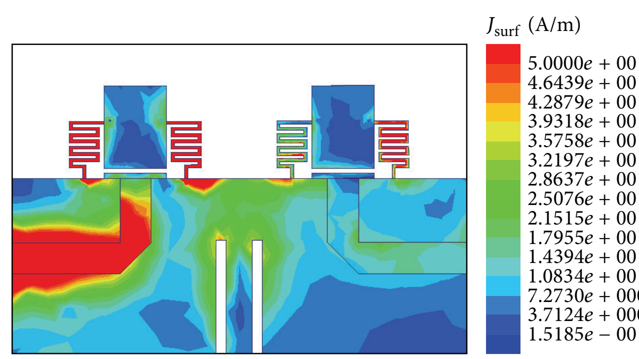

(b)

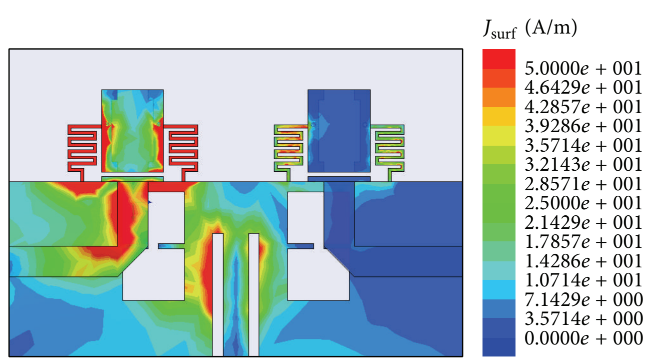

(c)

FIGURE 10: Surface current distribution at 2.44 GHz on metamaterial MIMO antenna (a) without DGS and (b) with the implementation of dual slots and (c) with full DGS.

antenna achieves high isolation coefficient which is less than −35 dB over all frequency of WLAN band while the operating bandwidth covers from 2.38 GHz to 2.52 GHz. The current distribution of the final MIMO antenna at 2.44 GHz is focused on the defected ground structure shown in Figure 10(c). Therefore, the effect of the surface current to the second element is significant reduced.

Simulated radiation patterns of final MIMO antenna in the xy, yz, and xz planes at 2.44 GHz when the antenna is fed; each port in turn is shown in Figure 11. The antenna displays

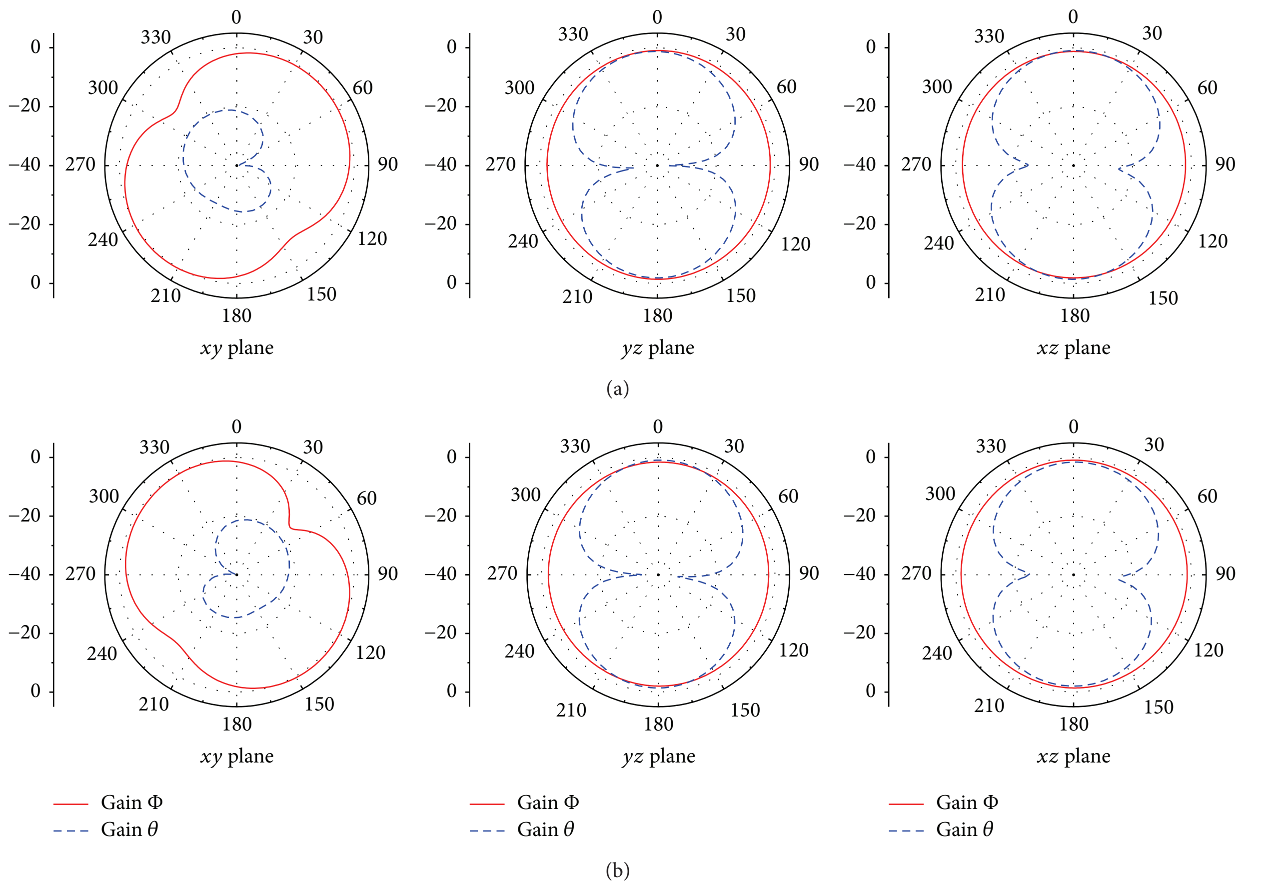

Figure 11: Radiation patterns of proposed metamaterial MIMO antenna at central frequency of 2.44 GHz when (a) excited Port 1 and (b) excited Port 2.

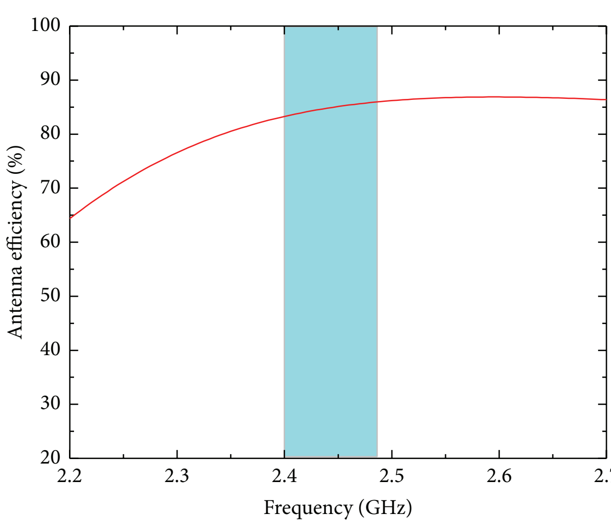

Figure 12: Simulated radiation efficiency of proposed antenna.

good omnidirectional radiation patterns in the yz and xz planes (H-plane) while the separate far field patterns are produced in the xy plane (E-plane). Therefore, the diversity for the antenna is achieved. Thanks to this characteristic, the antenna is a promising candidate for MIMO system.

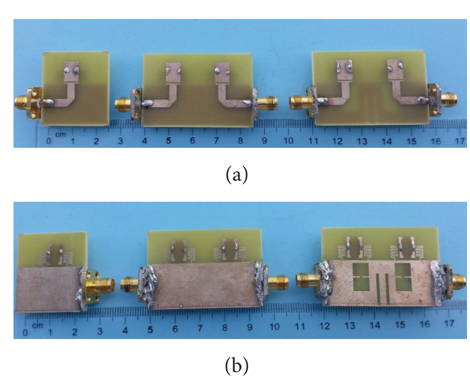

Figure 13: Fabrication of the single metamaterial antenna; initial and final MIMO antenna (a) front view and (b) back view.

Figure 12 gives the simulated radiation efficiency of the proposed antenna. This figure indicates that the proposed antenna shows good radiation efficiency, which has the average value of 85% in over the operating bandwidth of WLAN system.

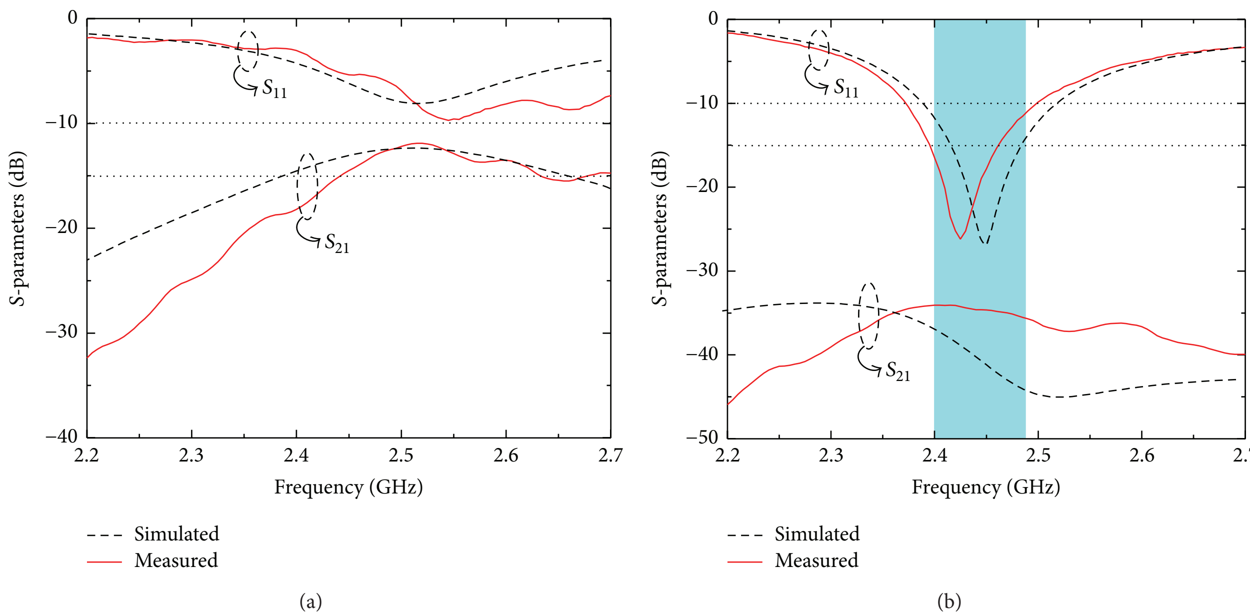

FIGURE 14: Simulated and measured S-parameters of (a) initial MIMO antenna and (b) final MIMO antenna.

Figure 14 presents the measured S_{11} and S_{21} of the fabricated initial and final MIMO antenna shown in Figure 13. From this figure, it is observed that the final MIMO antenna can operate over the range spreading from 2.38 to 2.5 GHz which is covering the WLAN band. Meanwhile, the mutual coupling between two elements (S_{21}) is less than −35 dB over WLAN range. It should be noted that the measured results are in good agreement with the simulated results.

3.3. MIMO Characteristics. MIMO antennas are required to be characterized for their diversity performance. In each system, the signals can be usually correlated by the distance between the antenna elements [16]. The parameter used to assess the correlation between radiation patterns is so-called enveloped correlation coefficient (ECC). Normally, the value of ECC at a certain frequency is small in case of the radiation pattern of each single antenna differently from each other. Otherwise, the same patterns of these antennas will exhibit the larger value of enveloped correlation coefficient. The factor can be calculated from radiation patterns or scattering parameters. For a simple two-port network, assuming uniform multipath environment, the enveloped correlation (ρ_e), simply square of the correlation coefficient (ρ), can be calculated conveniently and quickly from S-parameters [17], as follows:

$$\rho_e = \frac{\left|S_{11}^{*} S_{12} + S_{21}^{*} S_{22}\right|^2}{\left(1 - \left|S_{11}\right|^2 - \left|S_{21}\right|^2\right)\left(1 - \left|S_{22}\right|^2 - \left|S_{12}\right|^2\right)}. \quad (2)$$

The calculated ECC of proposed antenna by using the simulated and measured S-parameters is shown in Figure 15. From this figure, the proposed MIMO antenna has the simulated ECC lower than 0.01, while the measured one has lower than 0.02 over the operating frequencies. Therefore, the proposed antenna is suitable for mobile communication with a minimum acceptable correlation coefficient of 0.5 [18].

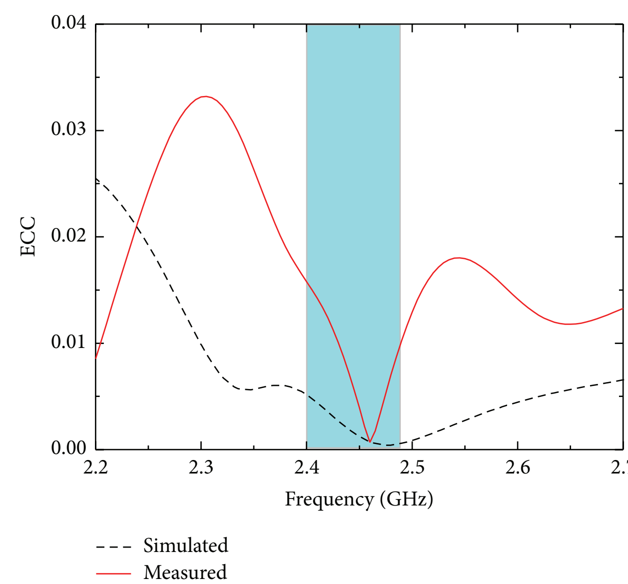

FIGURE 15: Simulated and measured proposed MIMO antenna's envelope correlation coefficient.

4. Conclusions

The compact 2 × 2 metamaterial MIMO antenna is designed to operate in WLAN frequency band. By using the modified CRLH model, the proposed metamaterial antenna achieves 60% size reduction in comparison with the unloaded antenna. The defected ground structures are inserted to suppress the effect of surface current on the elements of the proposed antenna for reducing the mutual coupling. The antenna offers the compact size with the diversity radiation patterns. The fabricated MIMO antenna shows isolation less than −35 dB over its operating frequency band spreading from 2.38 to 2.5 GHz. The proposed MIMO antenna has also a minimum correlation coefficient which is less than 0.02 over the WLAN frequency range. Summing up the result, it can be concluded that the proposed antenna is a good candidate for WLAN applications.

Conflict of Interests

The authors declare that there is no conflict of interests regarding the publication of this paper.

References

[1] J. P. Gianvittorio and Y. Rahmat-Samii, "Fractal antennas: a novel antenna miniaturization technique, and applications," *IEEE Antennas and Propagation Magazine*, vol. 44, no. 1, pp. 20–36, 2002.

[2] G. Monti, L. Catarinucci, and L. Tarricone, "Compact microstrip antenna for RFID applications," *Progress in Electromagnetics Research Letters*, vol. 8, pp. 191–199, 2009.

[3] W. J. Krzysztofik, "Modified Sierpinski fractal monopole for ISM-bands handset applications," *IEEE Transactions on Antennas and Propagation*, vol. 57, no. 3, pp. 606–615, 2009.

[4] A. Mehdipour, I. D. Rosca, A.-R. Sebak, C. W. Trueman, and S. V. Hoa, "Full-composite fractal antenna using carbon nanotubes for multiband wireless applications," *IEEE Antennas and Wireless Propagation Letters*, vol. 9, pp. 891–894, 2010.

[5] M. N. Jahromi, A. Falahati, and R. M. Edwards, "Bandwidth and impedance-matching enhancement of fractal monopole antennas using compact grounded coplanar waveguide," *IEEE Transactions on Antennas and Propagation*, vol. 59, no. 7, pp. 2480–2487, 2011.

[6] A. Arazi, "Ultra wideband fractal microstrip antenna design," *Progress in Electromagnetic Research C*, vol. 2, pp. 7–12, 2008.

[7] G. V. Eleftheriades, A. K. Iyer, and P. C. Kremer, "Planar negative refractive index media using periodically L-C loaded transmission lines," *IEEE Transactions on Microwave Theory and Techniques*, vol. 50, no. 12, pp. 2702–2712, 2002.

[8] G. V. Eleftheriades, "Enabling RF/microwave devices using negative-refractive-index transmission-line (NRI-TL) metamaterials," *IEEE Antennas and Propagation Magazine*, vol. 49, no. 2, pp. 34–51, 2007.

[9] G. V. Eleftheriades, A. Grbic, and M. Antoniades, "Negative-refractive-index transmission-line metamaterials and enabling electromagnetic applications," in *Proceedings of the IEEE Antennas and Propagation Society Symposium*, vol. 2, pp. 1399–1402, IEEE, June 2004.

[10] A. Sanada, M. Kimura, I. Awai, C. Caloz, and T. Itoh, "A planar zeroth-order resonator antenna using a left-handed transmission line," in *Proceedings of the 34th European Microwave Conference*, pp. 1341–1344, October 2004.

[11] M. A. Antoniades and G. V. Eleftheriades, "A folded-monopole model for electrically small NRI-TL metamaterial antennas," *IEEE Antennas and Wireless Propagation Letters*, vol. 7, pp. 425–428, 2008.

[12] A. Lai, K. M. K. H. Leong, and T. Itoh, "Infinite wavelength resonant antennas with monopolar radiation pattern based on periodic structures," *IEEE Transactions on Antennas and Propagation*, vol. 55, no. 3, pp. 868–876, 2007.

[13] J.-G. Lee and J.-H. Lee, "Zeroth order resonance loop antenna," *IEEE Transactions on Antennas and Propagation*, vol. 55, no. 3, pp. 994–997, 2007.

[14] J. Zhu and G. V. Eleftheriades, "Dual-band metamaterial-inspired small monopole antenna for WiFi applications," *Electronics Letters*, vol. 45, no. 22, pp. 1104–1106, 2009.

[15] J. Zhu and G. V. Eleftheriades, "A compact transmission-line metamaterial antenna with extended bandwidth," *IEEE Antennas and Wireless Propagation Letters*, vol. 8, pp. 295–298, 2009.

[16] A. Najam, Y. Duroc, and S. Tedjni, "UWB-MIMO antenna with novel stub structure," *Progress in Electromagnetics Research C*, vol. 19, pp. 245–257, 2011.

[17] J. Thaysen and K. B. Jakobsen, "Envelope correlation in (N, N) mimo antenna array from scattering parameters," *Microwave and Optical Technology Letters*, vol. 48, no. 5, pp. 832–834, 2006.

[18] M. P. Karaboikis, V. C. Papamichael, G. F. Tsachtsiris, C. F. Soras, and V. T. Makios, "Integrating compact printed antennas onto small diversity/MIMO terminals," *IEEE Transactions on Antennas and Propagation*, vol. 56, no. 7, pp. 2067–2078, 2008.